Next-generation Cryogenic Transfer and Autonomous Refueling (NeCTAR)

AggieSat Laboratory at Texas A&M University

AggieSat Laboratory Faculty Advisor: John F. Connolly, P.E. (AERO)
AggieSat Laboratory Program Manager: Shirish Pandam, B.S. (G, AERO)
NeCTAR Project Manager: Kamalika Bose, (UG, MXET)
NeCTAR Chief Engineer: Thomas Lopez, (UG, ESET)

NECTAR

NEXT-GENERATION CRYOGENIC TRANSFER AND AUTONOMOUS REFUELING

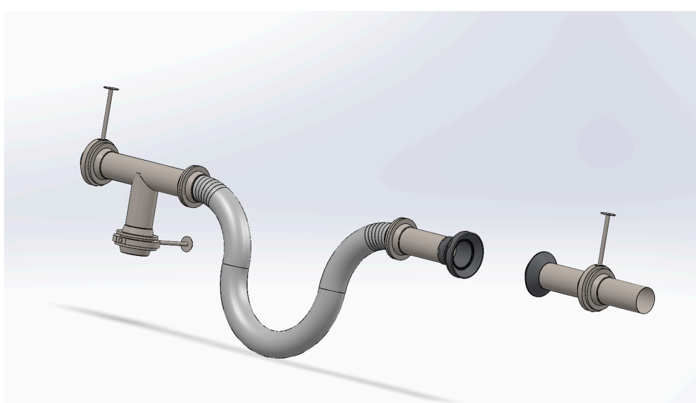

Faculty Advisor Signature :

NeCTAR Personnel

Thermals, Mechanics, and Structures
Lead: Kai Elmore, (G, AERO)
Ryan Chacko, (UG, AERO)
Miguel Cunanan, (UG, CPEN)
Arnav Shah, (UG, MEEN)

Electrical Power Subsystem
Lead: Pallavi Gokul, (UG, CPEN)
Melanie Fuentes, (UG, MXET)
Colter Swim, (UG, ENGR)

Command and Data Handling
Lead: Vincent Guerrero, (UG, AERO)
Ikaika Mendoza, (UG, CPSC)
Arthur Nguyen, (UG, CPSC)
Poorvi Parikh, (UG, ENGR)

Dynamics
Lead: Gage Wallace, (UG, AERO)
Sri Dhriti Kuram, (UG, CHEN)
Jaret Pinkerton, (UG, MXET)
Siquan (Cindy) Qiu, (UG, AERO)

Key
UG -Undergraduate
G - Graduate

AERO - Aerospace Engineering
CHEN - Chemical Engineering
CPEN - Computer Engineering
CPSC - Computer Science
ECEN - Electrical Engineering
ENGR - General Engineering
ESET - Electronic Systems and Engineering Technologies
MEEN - Mechanical Engineering
MXET - Mechatronics Engineering

NECTAR
NEXT-GENERATION CRYOGENIC TRANSFER AND AUTONOMOUS REFUELING

Texas A&M University - NeCTAR

Theme Category, Major Objectives & Technical Approach

- Autonomous Cryogenic Refueling Coupler
- Provide a sustainable autonomous solution that allows for fuel transfer to and from NASA's HLS on the lunar surface
- The approach is to have a coupler that autonomously makes contact and lock to NASA's HLS. Constant monitoring of pressure, temperature, and fuel flow rates increase the safety of the system. Low profile locking mechanisms and a full system purge after each cycle limit the invasiveness of the system, mitigating corrosion.

Image/Graphic:

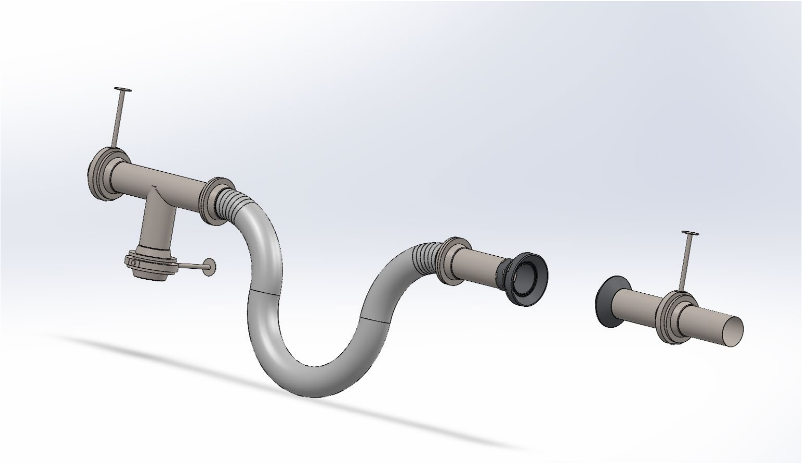

Key Design Details & Innovations of the Concept

- NeCTAR's design surrounds a gear rack driven flange that mates to a stationary flange located on NASA's HLS. The gear rack will provide tension between the flanges on O-rings to create a seal. Rather than using complex series of sensors and locks, NeCTAR will utilize a straightforward sensor suite to maintain telemetry and status as well as spring loaded linear actuators to create an inverted push/pull lock.
- Innovations include an electrodynamic dust shield (EDS) to "walk" regolith off of the coupler's surface, autonomous attaching/retracting, constant monitoring throughout each phase of refueling, and less invasive technologies.

Summary of Schedule & Costs for the proposed solution's path to adoption

- Schedule (Conclusions)
  - Assembly and Integration: 2.5 years
  - Environmental Testing: 3.5 years
  - Verification & Validation: 4.83 years
- Cost Estimates (x1000)
  - Components: $2351.4
  - Build, Integration, Test: $76289.27
  - Operations (Including Launch): $80,470.4

Table of Contents

1. Executive Summary

The Next-generation Cryogenic Transfer and Autonomous Refueling (NeCTAR) is an autonomous cryogenic coupler designed by AggieSat Laboratory at Texas A&M University to address key challenges in lunar cryogenic fuel transfer. Targeting NASA's goals for sustained lunar presence, NeCTAR provides a low-risk, scalable, and fully autonomous solution for bi-directional transfer of liquid oxygen. The system integrates structural dust mitigation, robust thermal regulation, and sensor-driven command and data handling to ensure safe, efficient operation over a 10-year mission life. NeCTAR reduces crew servicing needs, enhances safety in off-nominal scenarios, and supports future lunar and Martian refueling infrastructure. Its development advances NASA's cryogenic fluid management objectives, providing a viable path to adoption within 3–5 years.

2. Project Description

2.1 Background

Cryogenic fuel transfer in space poses a range of technical challenges due to both the extreme properties of cryogenic fluids and the harsh, microgravity environments in which they must operate. The behavior of liquid propellants under low-gravity conditions is particularly complex; in the absence of gravitational stratification, cryogenic fluids tend to form free-floating globules or adhere to tank walls due to surface tension, making it difficult to maintain a consistent flow during transfer operations [1]. These instabilities complicate the fluid dynamics within transfer lines and often result in unreliable delivery of fuel to propulsion systems.

In addition, the materials used to store and transfer cryogens must withstand severe thermal stresses. Cryogenic propellants can induce brittleness, fatigue, and cracking in conventional structural metals, especially when exposed to repeated temperature cycles or contact with subcooled liquids [1]. Even slight deviations from optimal thermal conditions can trigger flash evaporation, leading to the formation of vapor bubbles and vapor locks—conditions that can halt transfer processes and endanger system integrity [1].

Perhaps most critically, the handling of cryogenic fluids introduces significant safety and contamination risks. Improperly managed systems may suffer from leaks, pressure buildup, or even explosions. Over long-duration missions, these risks are amplified by the potential accumulation of residual gases and lunar regolith from plume-surface interactions (PSI), which can obstruct transfer lines or damage internal surfaces [1]. These issues present serious obstacles to NASA's objectives for sustainable lunar exploration.

To ensure the viability of future missions, solutions must address these multifaceted challenges through automation, robust material selection, thermal control, and reliable docking interfaces. Enabling safe, autonomous cryogenic refueling is not only critical for the Artemis program but also foundational for future crewed missions to Mars.

2.2 Design Constraints

The primary design constraint for NeCTAR falls in the mass and size of the system in its entirety. The system must be able to travel to the moon given current NASA transport systems and be easily assembled on the lunar surface given standard EVAs. Preassembled sections of the system allow for easy transport and assembly given the constraints presented solely by being a lunar system.

Due to the necessity for a section of external pipeline for NeCTAR's operation, unique design constraints were taken into consideration. Firstly, the pipeline must have a flexible hose section to allow for linear motion during the mating procedure between the coupler and the ship. This hose must be able to withstand the force of the fuel flowing through it, maintain material integrity while exposed to lunar PSI and low temperatures and pressures, and be constructed of a low-weight material to allow for transport and implementation on the lunar surface.

The linear actuators must be able to withstand repeated use over time. Additionally, linear motion is controlled via three gear rack and pinion assemblies. These assemblies must be able to withstand the mass of the system and efficiently move the coupler to and from the ship during the refueling operation. These gear rack and pinion assemblies must also be able to withstand any offset that the system may compensate for due to any abnormal positioning of the ship that is to be refueled. This includes material strength to withstand any flexing and accurate positioning inputs via limit switch to prevent any undershoot or overshoot when mating the coupler to the ship.

The flow rate for NeCTAR's system is controlled through a series of butterfly valves. These butterfly valves must have the ability to be controlled via servo motors embedded in the top of each valve and be able to withstand the pressure of the fuel pushing on the valve's switching surface. These butterfly valves must also fit the entire diameter of the pipe to prevent any leakage and be rated for cryogenic fuel to maintain structural integrity. The bidirectional nature of NeCTAR places key positioning requirements for these butterfly valves to ensure proper refueling operations.

2.3 Post-Proposal Amendments

The primary change done to the NeCTAR's design post-proposal was the introduction of a flared flange. This change allows for a lower risk yield during the refueling process, making it easier for the coupler to mate with the ship. Additionally, spring loaded O-rings were added to create a stronger seal at the mating location, with internal springs pushing out on the O-rings to force a stronger seal and increase the lifespan of the O-rings as they are more susceptible to damage through contact over time and refueling repetitions. Additional developments were made in material selection throughout the design to improve weight constraints and lifespan.

2.4 Next Generation Approach

NeCTAR stands to implement innovative technologies in its design through autonomy. Machine learning is a crucial aspect of this project in recognizing the patterns that come with refueling on the lunar surface. The computer will recognize inputs set through limit switches and flow rate sensors to follow a standardized refueling process, removing the constant need for human interaction. Nominal operations will utilize a similar structure for each iteration of refueling, allowing the computer to recognize any anomalies throughout the refueling process. Once an anomaly is recognized, different abort processes and system checks will be done to ensure safe and continued operation of the system. The physical design of NeCTAR compliments the autonomy of the system, allowing the male and female portions of the system to dock correctly and seal via linear actuators to create a less invasive docking technique, increasing the lifespan of the system and reducing the possibility of catastrophic error.

2.5 System Overview

2.5.1 Thermal, Mechanics, and Structures (TMS)

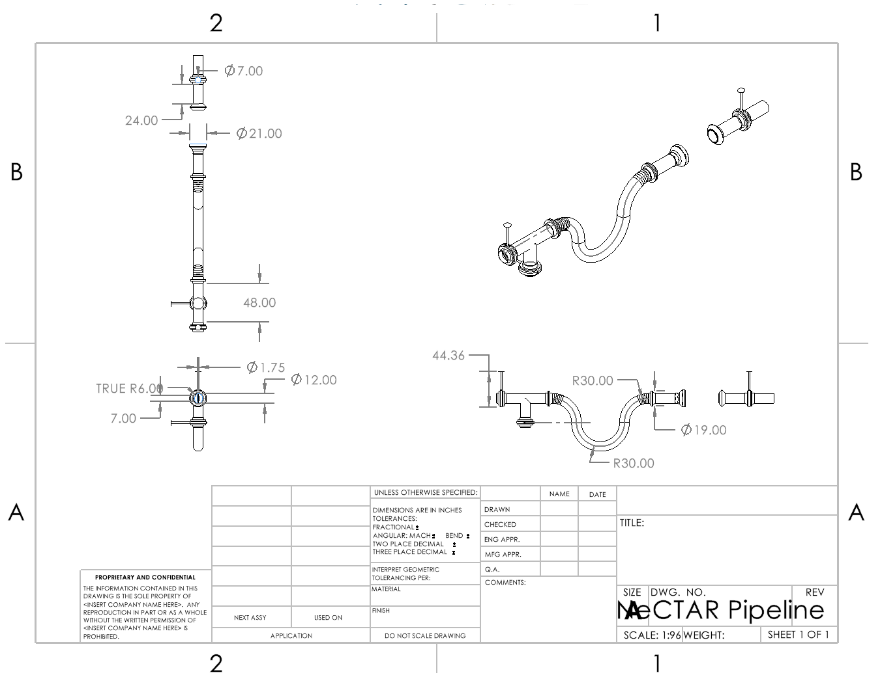

Figure 1. NeCTAR Pipeline Engineering Drawings.

The foundational operating principle of NeCTAR is contained in the design of the pipeline itself, designed by the TMS subteam, optimized for the Moon's vacuum, enabling passive thermal isolation and minimizing convective losses. The first challenge identified and approached by the TMS subteam was to prevent lunar regolith intrusion into the cryogenic propellant system and surface adhesion onto critical transport hardware, driven by both mechanical abrasion and electrostatic attraction. The second challenge was achieving autonomous mechanical coupling and precise alignment between fluid interfaces, accounting for positional tolerance, actuation reliability, and unassisted operation. The third was enabling bidirectional cryogenic fluid transfer under vacuum, thermal, and gravitational constraints inherent to the lunar environment. The final challenge was maintaining thermal and structural stability, primarily across extreme temperature gradients caused by cryogenic propellants, but also across radiative exposure on the lunar surface.

Regolith intrusion and adhesion must be mitigated by preventing mechanical infiltration and countering electrostatic forces. Due to the Moon's lack of atmosphere and erosion, lunar dust is fine, sharp, and highly abrasive. Solar Ultraviolet (UV) and solar wind exposure electrostatically charges both the dust and surfaces it adheres to [2][3][4]. A London-like adaptation predicts localized magnetic fields on the order of 10^{-10} T—several magnitudes above planar Biot–Savart estimates (~10^{-16} T)—due to surface curvature and charge gradients [5][6]. Though extremely small, these fields are comparable to lunar crustal anomalies and may passively reduce dust adhesion near sensitive coupling interfaces [5][6].

A localized Yttrium Barium Copper Oxide (YBCO) coating is applied at the coupler interface and maintained below its 90 K superconducting transition using adjacent liquid oxygen flow. YBCO was selected over coatings such as MgB_2, NbTi, and Nb_3Sn for its higher operating temperature, mechanical resilience, and cryogenic integration maturity [6]. YBCO coatings, applied as thin-film superconducting oxides, exhibit mass stability within 0.00014% across critical temperature phase transitions and ELF exposure [6]. Their outgassing behavior aligns with inert ceramics like Al_2O_3 and Y_2O_3, both ASTM E595-qualified. With a London penetration depth of ~53 nm, YBCO supports persistent surface currents that establish a Meissner exclusion zone, passively repelling charged particles [5]. Applying the London relation with a calculated current response factor of 2.81×10^{20} A·s/(kg·m²), the resulting passive field stabilizes the local electrostatic environment and protects nearby sensors [5].

Surrounding the superconducting core, an active dust-repulsion system is embedded along the female flared flange. It uses noncontinuous concentric rings of nickel-plated copper electrodes—selected for cryogenic conductivity and corrosion resistance—driven by a high-voltage H-bridge circuit that alternates polarity at controlled frequencies [8]. The resulting pulsed electric field destabilizes dust adhesion and repels charged particles during coupling [8][9][10][11]. The remainder of the fluid system, including pipes, valves, and structural supports, is built from 316 stainless steel to maintain weld consistency, thermal stability, and mechanical integrity [12].

Autonomous mechanical coupling is achieved via linear actuation from the ground pipeline to the vehicle umbilical, constrained to a single degree of freedom. The system uses three (3) synchronized rack-and-pinion drives, each powered by dual motors driving a 20-tooth, 3-inch pitch gear (24° pressure angle). These mesh with 60-tooth, 9-inch pitch gears for torque amplification, which transmit motion through a 30-tooth, 2.63-inch intermediate gear to a final 45-tooth, 3.95-inch pinion that interfaces with the rack. Each unit delivers ~1,566 lb-ft of torque, totaling 4,698 lb-ft across all three systems. The resulting calculated 5.7-foot linear travel accommodates the required kinematic alignment slack, ensuring reliable coupler engagement during docking.

Three cryo-rated butterfly valves are positioned at key junctions to regulate bidirectional fluid transfer: one at the inlet near the electronics mounting zone (fill line), one beneath the pipeline (drain), and one just upstream of the coupler interface at the vehicle side. These valves meet reliable operation below –195 °C, ASME Class 300 standards, and provide low-torque actuation, compact footprint, and fast switching for docking sequences [12].

The pipeline is wrapped in a multilayer insulation (MLI) of alternating double aluminum-coated Mylar and Dacron spacers, per NASA-CR-134411 guidance for thermal protection in space applications [13]. Outer layers incorporate Cryolite, which provides impact resistance and low conductivity. The fluid line is concentrically suspended within a one-inch (25.4 mm) vacuum jacket; within this annular space, a 1/8-inch pipe embedded with electronics runs along the interior wall for passive heat rejection.

Feedthroughs are precision-machined through both the MLI and Cryolite to permit Gas Tungsten Arc Welding (GTAW), or TIG welding, of pressure and temperature sensors directly into the system at two critical locations: upstream of the inlet valve and at the coupling interface region. Their construction, including adhesives and metal interfaces, is selected to manage cryogenic contraction and meet ASTM E595 outgassing criteria for low total mass loss (TML) and collected volatile condensable material (CVCM) [14]. Stainless steel standoffs (6–10 mm diameter) are perpendicularly mounted to the inner pipe and covered in MLI to allow monitoring without disturbing flow or insulation.

To meet aerospace standards for structural and thermal stability, the design incorporates custom 37.5° flared flanges—machined via manual or CNC lathes—for passive centering and uniform O-ring compression under axial approach. This flare angle, aligned with SAE J514, enhances fatigue resistance, sealing repeatability, and alignment under pressure cycling [14]. Flange joints use cryo-compatible elastomeric seals validated under NASA ASTM E595-15 (TML < 1.00%, CVCM < 0.10%) [14], with groove and sealing geometries conforming to SAE AS568 and AS5857 [16][17]. O-ring glands are precision-machined per AS568 to ensure consistent sealing and reusability [16].

The cryogenic conduit uses a 1-inch-thick PCTFE film, which was selected for its cryogenic tensile strength (127.78 MPa) and modulus (5.65 GPa at –196 °C). PCTFE was chosen from a trade study among fluoropolymers tested for liquid oxygen transfer due to its flexibility and durability in harsh thermal conditions [18][19][20]. Flange-to-pipe joints are gas tungsten arc welded (GTAW) in accordance with AWS D17.1 and NASA-STD-5006A, following pre-machined bevel geometries to ensure full penetration and repeatability [21][22][23].

The flared flanges are made from Titanium-Zirconium-Molybdenum (TZM), selected through a trade study of aerospace-grade materials including Invar, 316L stainless steel, Teflon, Beryllium Copper, and Nickel Steel. TZM offers high cryogenic strength (~690 MPa), low thermal expansion (~5.1 µm/m·K), and moderate thermal conductivity (~125 W/m·K), with strong compatibility for superconducting interfaces and LOx environments [24][25][26]. Alternatives like Ti-6Al-4V and Inconel 718 were considered but deprioritized due to inferior thermal performance and integration challenges.

2.5.2 Dynamics (DYN)

The DYN subteam approached the characteristics and behaviors surrounding the flow of cryogenic fluids throughout the system, working closely with TMS to focus on their primary objectives: to maintain an optimal cryogenic environment in the system, develop a flow path capable of bidirectional flow while ensuring no backflow may occur, and ensure the coupler system may attach and detach in a simple and repeatable manner for the onboard computer.

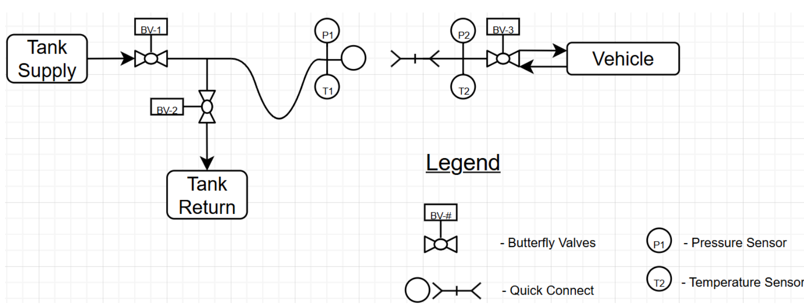

Figure 2. NeCTAR Piping and Instrumentation Diagram.

The pipeline design chosen for NeCTAR, shown above in Figure 2, involves a pad section (left of the coupler) and a vehicle section (right of the coupler). On the pad section, there are two separate pipelines. The first is the fill line, designed for fuel to flow from the supply tanks to the vehicle, and the second is the drain line, designed for fuel to flow from the vehicle to the return tanks. It should also be stated that there are other systems needed for this pipeline that are not included. Systems such as the propellant farm tanks on the lunar surface, pumps to supply the fill pressure, and check valves to prevent backflow in either of the two lines. These were not included because they were determined to be outside the scope of the coupler system. The next critical aspect of NeCTAR's pad section is the bent hose line. This system was chosen to allow for the extension of the coupler section for attachment and detachment.

The development of a bi-directional cryogenic coupler relies heavily on the valve selection to ensure reliable and precise control of the fluid flow. After evaluating a variety of valve types, cryogenic rated butterfly valves were decided upon for optimal fuel regulation. A few technical requirements for a cryogenic valve system include reliable operation at temperatures below -193℃, easy integration with the insulation system, low torque operation, and lightweight design. Butterfly valves are significantly more compact than other valve designs and require a much lower actuation torque, meaning less power usage for the system in comparison to other valve designs [27]. This also requires smaller electric actuators, allowing easier integration with the insulation system. Butterfly valves are particularly useful for bi-directional flow due to their fast actuation and linear flow regulation characteristics [27]. For the NeCTAR system, these valves will be operational at temperatures of -195℃ and rated ASME class 300, meaning it meets both the temperature requirements and pressure requirements [27]. The valve itself is designed to encompass the diameter of the pipe (12 inches). It is made with stainless steel, identical to the rest of the piping.

Multiple pipe diameters were looked at for the cost analysis section, however, the main design moved forward with a 12-inch pipe diameter. The 12-inch diameter was chosen to supply a very large flow rate to fill Starship, the largest vehicle currently planned to land on the lunar surface, in just over half an hour. The solid and hose piping will both be made of stainless steel. Although not the lightest weight, stainless steel is the most viable material in cost and chemical compatibility. The hose was decided to be a 12” single braided stainless steel hose capable of withstanding down to -195℃ and up to 200 psi, meeting the environment requirements of the line. The thickness of the solid steel pipe was then chosen to be a minimum of thickness of 1/32” from hoop stress calculations based on the MAWP; however, for structural integrity, a thickness of 1/8” was determined acceptable.

The main connection of the NeCTAR system is the coupler itself, with many considerations. The coupler connection was decided to be a flared flange connection. The flange was decided for simple connection, as well as a flange being one of the few detachable connections for large diameter pipes. The flare was added to give a margin of error for a coupler navigation system. The rest of the connections for all the valves in the system were determined to be simple ASME 300 class flanges, as that is what the sourced butterfly valves require.

With all connections being flanges, seals become the most critical component of the pipeline. Seals also exhibit the most challenging restraints, they must be reusable for cyclical connections and cryogenic rated. These two requirements in tandem knock out many common O-ring seals, leading to the decision of spring-energized PTFE O-rings. Such O-rings exhibit an external PTFE wall with a stainless steel spring coiled inside. PTFE provides a chemically compatible base capable of operating down to -195℃. However, regular PTFE O-rings are permanently deformed when used and thus not reusable, this leads to the need for the inner spring. The spring inside these seals provides an outward force when the O-ring is compressed, preventing permanent deformation and thus allowing these seals to attach and detach for the coupler application.

To minimize thermal losses and maintain the integrity of the cryogenic fluid, especially in the lunar environment, a high performance insulation system is necessary. The proposed system entails the use of vacuum jacketed piping, combined with multi-layer insulation (MLI) and a Cryolite outer shell for protection against radiation and the cold lunar temperatures. Assuming the temperature of the inner pipe is at -193℃ (which will be explained later in this report), this insulation system is multi-functional for the cryogenic fluid as well as the electronic systems inside the piping [28].

The cryogenic pipeline consists of two concentric pipes, an inner pipe (containing the fluid) and the outer pipe. Between these pipes lies the vacuum annular space. This system eliminates convective heat transfer and drastically reduces conductive heat transfer [29]. Using an industry standard assumption that the section of the pipeline containing th bi-directional coupler will be within the volume of 18.3 m^3, the gap between the two layers of pipe was calculated to be 26 mm [29]. This means there is 26 mm of pure vacuum insulation (disregarding the MLI and cryolite layers) [29]. This vacuum jacket will wrap around the entire system including the hose, valves and actuators.

The second component of the insulation system was selected to be a combination of the multi-layer insulation (MLI) with Cryolite. The MLI was composed of a minimum of 20 layers, including the aluminized beta cloth as the outer layer, double aluminized mylar as the reflector layer, dacron netting as the spacer, with the Cryolite blanket attached on the cold side of the MLI. Aluminized beta cloth serves as the outer layer of the MLI system, designed to reflect maximal direct radiation from the heat source. Aluminized beta cloth was chosen for its thickness and environmental standards, .020 cm/layer compatible with AO, Atomic Oxygen, and UV Radiation. Past flight uses are: EOIM-3, and the ISS. Double aluminized mylar serves as the reflector layer for its emissivity and thickness, Infrared Emittance of .05; .03, and a thickness of .0051-.127 mm. Aluminized mylar has been adopted as a part of the Apollo Lunar Module CGSS and Apollo 9 mission. Dacron netting serves as the spacer for its low heat flux and inverse knudsen number, corresponding to low conductivity and better insulation performance to alternative materials. Dacron netting has been adopted as a part of the Perseverance rover's thermal blankets to Mars. Dacron netting was chosen for its thickness and weight, .16 mm (plus or minus .01 mm) and 6.3 gram/m^2 (plus or minus .85 grams/m^2).

Considering a maximum 40 layer count: Total outer insulation thickness (MLI + Cryolite): 64.5 mm. Studies show that the 40 layer MLI with Cryolite combination outperforms the MLI system alone, with a lower percentage of heat leak. Cryolite is easy to install, has low layer density, compatible with oxygenated conditions, and helps to maintain a stable vacuum. Test shows placing Cryolite on the cold side of the MLI enhances the thermal performance of the overall insulation system, especially for gas conduction, providing elasticity to reduce edge effect and evacuation between layers to remove trapped gases. Additionally, studies show layer by layer interleaved joints and overlap joints are recommended for MLI assembly to minimize heat leak.

Reliable operation of the system is dependent on the electronic components such as the actuators, sensors, circuits and communication modules. These components must be protected from extreme temperatures, radiation, dust and vacuum present on the moon. Therefore this system utilized a two-tiered protection strategy with all of the electronic components placed inside the vacuum jacket with a protective/insulated outer piping that wraps around the component [31]. The seals and metals used in the piping and insulation will be protective against lunar dust [30].

Monitoring the temperature and pressure within the inner cryogenic pipeline is essential to regulate safe fluid flow. Therefore, a specialized sensor interface is integrated into the inner pipe of the vacuum jacketed system. A small sensor tube, or sensor probe standoff will be welded into the inner pipe. This tube will stand vertical (perpendicular to the inner pipe) and will stay underneath the outer piper to still be protected by the insulation systems. Sensors to measure the pressure and temperature of the flow will be mounted at the top/end of this tube, with wiring attached to the other end of the sensor. The tube itself will be narrow, around 6-10 mm in diameter, made of stainless steel for integration with the rest of the piping [32]. The tubing will be thin walled and covered with MLI so that the sensor placement will not impact or disrupt the flow of the cryogenic fluid [32].

2.5.3 Electrical Power Subsystem (EPS)

The goal of the EPS is to create an efficient electrical system that reliably generates, distributes, and maintains adequate power to subsystems, to ensure that all electrical components are capable of reliable, long-term usage in vacuum and cryogenic conditions, and to develop an effective communications system for the coupler's sensors and actuators.

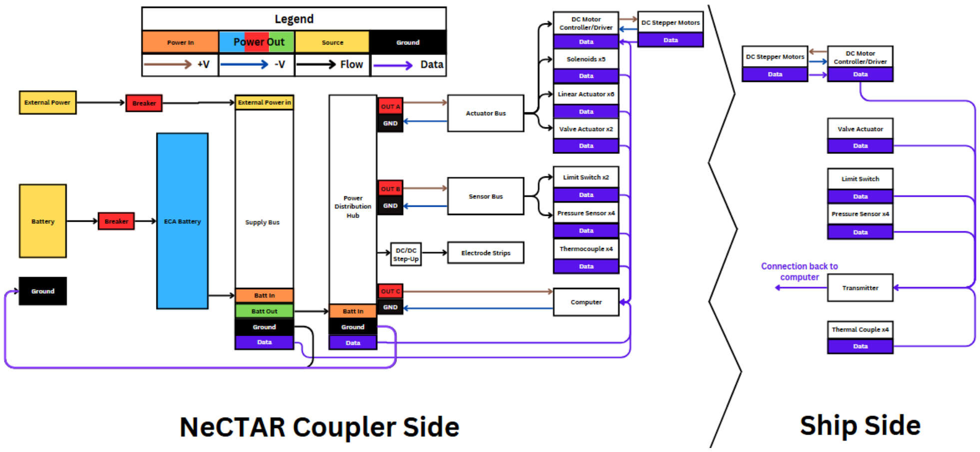

Figure 3. EPS Functional Block Diagram.

The EPS is divided into two different parts, shown above in Figure 3, maintaining a presence on both the coupler side of the system and the ship side. On the coupler side, the EPS begins at the power supply, where a 91-cell battery is located. A circuit breaker is included to protect the rest of the system from sudden surges. The power supply then feeds into an electrical control assembly battery, which in turn supplies stabilized DC power to the supply bus through the battery in port. From the supply bus power goes into the power distribution hub (PDH), which segregates and routes the power to three channels: the actuator bus, the sensor bus, and the dust protection mechanism, and to a transponder for the data. For the dust protection the power first goes through a DC-DC Step-up before entering the electrode strips in order to supply the electrode strips with a stronger current. Metering occurs at every stage of the EPS to monitor the system and observe any discrepancies that occur. All of this information is fed back into a computer. The same actuators and sensors that are present on the coupler side are on the ship side other than the linear actuators and the solenoids. Like on the coupler side, metering occurs at every stage. The information is fed into a transmitter which connects back to the computer.

System	Component	Manufacturer	Model	Power (W)	Voltage (V)	Current (A)	Quantity	Total Power (W)
	Temperature Sensor	Lake Shore Cryogenics	Cernox-HT (CO)	N/A	N/A	N/A	8	0
	Pressure Sensor	PCB Piezotronics	102M81A (15-30V)	0.56	28	0.02	8	4.48
Sensor Array	Limit Switches	Sensata Technologies	4AT64	112	28	4	3	336
	Valve Actuators	Lin Engineering	5718L-01P	67.2	24	2.8	3	201.6
Actuators	Linear Actuators	Lin Engineering	8718L-08P-Y05-A0-A24F	369.6	48	7.7	6	2217.6
	Electrode Sheets	MSE Supplies	MSE PRO High Conductivity Carbon Nanotube Film	22.5	300	0.075	1	22.5
Dust Protection	H-Bridge			0			1	0
	Transponder	L3Harris	CXS-1000	19.6	28	0.7	1	19.6
Transmitters/Recievers	Transmitter	ISISPACE	S-Band Transmitter	30	20	1.5	1	30
Stepper Motor Controller/Driver	Driver/Controller	Lin Engineering	R256	48	24	2	9	432
Vacuum Solonoid Valves	Solonoid	Sintered Metal Corporation	XSA NC Straight Solonoid Valve	4.5	12	0.375	5	22.5
Total Wattage:			3286.28		Total Voltage:		Total Components:	
					500		46	

Figure 4. NeCTAR Power Budget.

The NeCTAR battery system is responsible for providing voltage to the system with the help of a DC-DC step-up boost converter. The converter will increase the voltage to a higher level and power the components. The battery system is a 91-cell battery consisting of thirteen 3.7 volt batteries in series and seven 3.7 volt batteries in parallel. This power system was developed to accommodate the power budget set by NeCTAR, shown above in Figure 4.

The NeCTAR system sensor bus is responsible for the power distribution to four pressure sensors and two limit switches. In addition, there will be four thermocouples. Two cryogenic rated pressure sensors and two cryogenic rated thermocouples will be placed in either cryogenic line (two in the fuel line, two in the oxidizer line). The pressure sensors will monitor the flow of the fuel to detect leaks or anomalies with the flow rate. The thermocouples will monitor the temperature within the system so it stays within operational limits. The limit switches will be placed on the front end of the NeCTAR coupler to determine the position of the coupler and ensure that it does not overextend. On the ship side of the system an additional limit switch, four pressure sensors, and four thermocouples will be present to ensure that the coupler mates successfully and that the pressure and temperature are within operational limits on both sides of the system.

The system will also incorporate an actuator bus responsible for distributing power to five solenoids, six DC stepper motors serving as linear actuators, two DC stepper motors serving as valve actuators, and the DC Motor Controller/Drivers which serve as H-Bridges. The linear actuators will specifically be used to control the movement of a gear train that allows the coupler to move back and forth so it can mate with the ship side fuel tank. The valve actuators' specific role is to control the butterfly valve. Together, the stepper motors will have their data lines connected to the Motor Controller/Drivers, allowing for precise control in either direction and accurate positioning data for the system. The ship side will contain one stepper motor and one motor controller, both for the purpose of valve actuation, allowing the cryogenic fuel to transfer in either direction.

The NeCTAR system will incorporate an electrostatic dust mitigation mechanism. The exterior of the coupler will be lined with an electrode sheet, across which a high voltage will be applied to generate a strong electric field at the coupler surface. This field repels charged dust particles and will minimize dust adhesion. A high voltage H-Bridge circuit will be used to alternate the polarity of the applied voltage, which will aid dust removal. A DC-DC Step-Up converter will be used to boost the voltage as needed to generate a strong enough electric field.

2.5.4 Command and Data Handling (CDH)

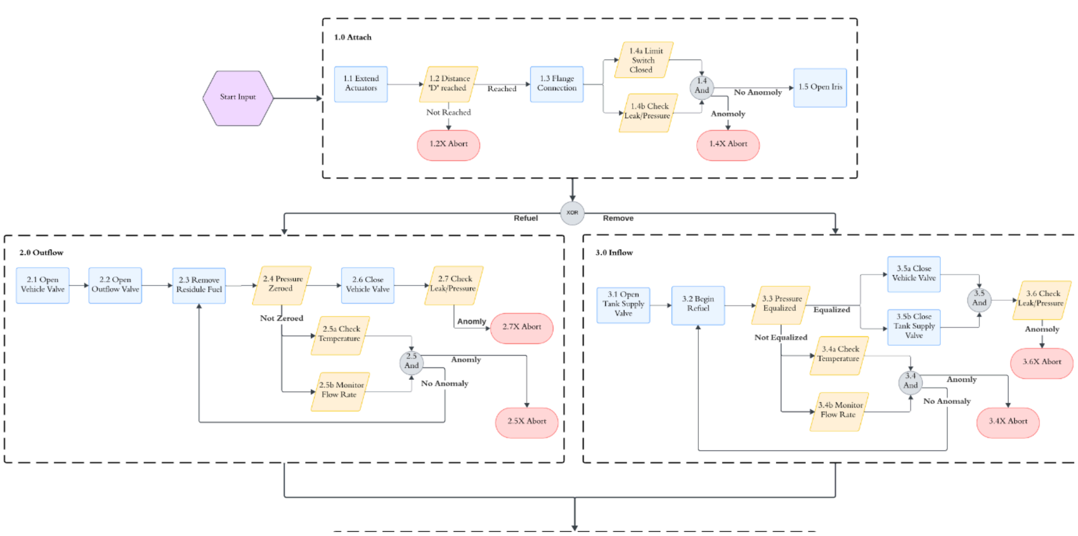

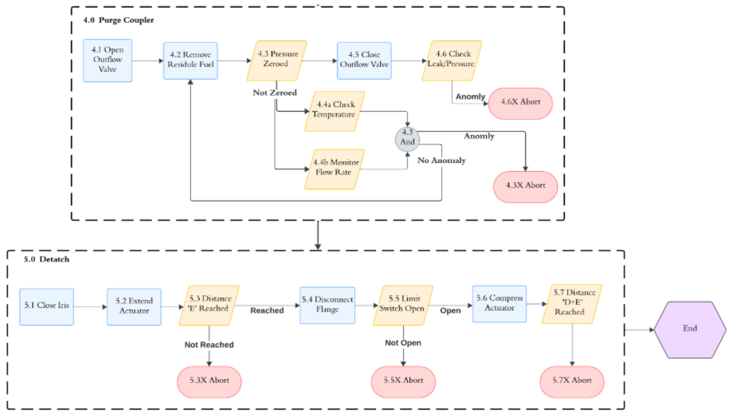

Figure 5. CDH State Diagram.

The CDH subsystem performs computational analysis to support autonomous diagnostics and real-time decision-making for NeCTAR. Developed via a State-Flow diagram, the framework provides an overview of each system stage, as shown above in Figure 5, and highlights key decision points and constraints. The start/end points are represented by purple hexagons at the beginning of *Mainstage 1.0* and end of *Mainstage 5.0*. Procedures are marked by blue rectangles, conditionals by yellow rhombuses, and aborts by red ovals. Logical operators are shown as grey circles for simultaneous operations and checks.

Mainstage 1.0 Attach ensures the coupler is securely connected to HLS. The process begins by extending the linear actuators to a distance *D*, calculated based on the distance to the target. If the distance is not reached, the process aborts and returns to the initial state. If successful, the stage moves to the flange connection process. Two conditions must be met: the limit switch must be closed, and the seal must be stable. The limit switches lock the mating hardware when contact is made. If conditions aren't stable, the process aborts. Once all parts are connected, the internal iris opens, and the system initiates *Mainstage 2.0 Outflow* (if transferring fuel to the fuel farm) or *Mainstage 3.0 Inflow* (if refueling the vehicle).

The next two stages begin fuel transfer. *Mainstage 2.0 Outflow* moves fuel from HLS to a storage tank, while *Mainstage 3.0 Inflow* refuels the vehicle. Once a stable connection is present, the vehicle's valve and NeCTAR's outflow valve open, starting fuel removal or supply. The sensor suite tracks the HLS tank volume, temperature, and flow rate allowing accurate fuel transfer through pressure differentials. If anomalies occur, the system aborts to prevent leaks or fluid multistates. This process runs until the pressure equalizes. Once fuel is fully transferred, the vehicle valve is closed, and pressure is monitored. An anomaly in pressure will abort the process, and *Mainstage 4.0 Purge Coupler* is initiated if no issues are detected.

Mainstage 4.0 Purge Coupler removes residual fuel from the coupler after transfer. If *2.0 Outflow* was used, the outflow valve is open; otherwise, it opens in *Mainstage 4.0*. A non-zero pressure difference indicates residual fuel, triggering monitoring of temperature and flow rate. Any anomalies cause an abort. The process continues until the pressure differential reaches zero, indicating all fuel is removed. The outflow valve closes, and pressure sensors check for leaks. An anomaly results in abortion, and *Mainstage 5.0 Detach* begins.

Mainstage 5.0 Detach retracts the arm and resets the coupler. The iris closes to protect against contaminants, and actuators retract to disengage the locking mechanism. The limit switch is checked for a positive disconnect, which allows the actuator to retract to its standby position. If the retracted distance is incorrect, the process aborts and the system is checked. A successful nominal check completes the cycle.

3. Verification and Validation

3.1 Solution Verification

Verification and Validation for NeCTAR falls under two main categories, one that is primarily the physical operation of the system determined by CDH and EPS, and another that is primarily the fluid properties of the system determined by DYN and TMS. All subsystems are also tested together to ensure nominal operation of the system as well as proper implementation of failsafes should they be needed.

The CDH state diagrams follow all possible inputs and respective outputs of the system during the refueling process. The VV plan for CDH involves running a software simulation of the system under various conditions to ensure that signals are processed and sent to their intended destination. Initial setup includes a target signal sent to the computer for a target acquisition and system initialization. From there, values are set to mimic the extension of the coupler, successful mating, and fuel flow both to and from the target to ensure bidirectional flow in the system. Different flags can be raised to simulate anomalies. A small scale prototype is used in conjunction with this software simulation to ensure that the EPS is compatible with the respective commands sent by the CDH subsystem.

The VV plan for the TMS subsystem involves stress analysis under the minimum, nominal, and maximum conditions that the system could experience. CAD models of the full-scale system have been developed and are to be used in conjunction with the DYN subteam to simulate loading, fluid flow, and external anomalies that come from operating on the lunar surface. The VV plan for DYN also entails utilizing operating conditions as they relate to temperature and other environmental factors to ensure the flow rate and fluid characteristics maintain a stable condition throughout the refueling process.

All subsystems fall under a full-scale VV plan to ensure entire system success under a variety of different conditions, including but not limited to bidirectional flow, limiting systems to prevent overflow, extension and retraction of the coupler, coupler docking at an offset, system purging, system aborts, and full-cycle refueling operations. These conditions take into account valve control, abort procedures, system calibration, anomaly detection, and standard operating procedures.

3.2. Obstacles in Development

Under the VV plan, several obstacles are highlighted and used to analyze the risks associated with the system. Lunar PSI is a large risk for the system, with high velocity particles posing a large risk for system punctures and instability throughout the refueling process should they go unnoticed. This is addressed by implementing an electro-static dust shield across the system that utilizes a charged surface to repel any regolith that comes into contact with the system. Additionally, an iris is located at the coupler ends to protect the internal structure of the system from damage and contamination. Another obstacle comes from the alignment of the coupler itself with the ship side of the refueling operation. Because NeCTAR is a static system, leeway is needed to allow the system itself to flex to accommodate any offset in coupler alignment. This was addressed through material selection and is further tested under the TMS VV plan. Linear alignment is addressed via the limit switches sensing positive contact to alert the linear actuators to halt any motion and begin the sealing process. The final major obstacle comes from the construction of the system itself, with the final size and mass of the system posing risk at launch and during construction. Material selection and the ability to create preassembled sections of the system address these obstacles.

4. Technological Assumptions

NeCTAR assumes the following conditions for both its path-to-flight and operations on the lunar surface.

1. Pre-existing infrastructure on the lunar surface is readily available to include a fuel farm, fuel supply tanks, a standardized pipeline to and from NeCTAR's respective supply and return, and a landing pad or dedicated refueling location for staging.
2. NASA's SLS and/or HLS is capable of dedicating space for the transportation of NeCTAR in preassembled sections at the discretion of the agency and commercial partners.
3. NeCTAR will be assembled on the lunar surface through standard EVA construction practices.
4. The cryogenic conditions that NeCTAR shall operate under will be a temperature of -193℃, allowing for liquid oxygen, liquid methane, and liquid natural gas applications under a maximum allowable working pressure of 186 psi.
5. The cryogenic fuels that NeCTAR will be subjected to will be standardized fuels that are to be used under NASA's HLS as determined by the agency.

5. Mass and Size

The bulk of NeCTAR's mass stems from the materials embedded in the pipe itself, as well as the coupler assembly. The structural pipe system, made from 316 stainless steel, maintains an approximate total mass of 1293.56 kg. The custom-flared male and female flange assemblies, machine from TZM alloy, have respective masses of 305.39 kg and 177.96 kg. The three triple-offset cryogenic butterfly valves have a mass of 64.8 kg each, with a total mass of 194.4 kg for the assembly. The PCTFE cryogenic liner comes to a total mass of 15 kg. The electronic components take up a much smaller portion of the mass, with the pressure sensors having a total mass of 0.044 kg, linear actuators having a total mass of 33.53 kg, valve actuators having a total mass of 3.19 kg, and a margin of 10 kg for wiring and components with miniscule mass throughout the EPS.

6. Path-to-Flight Timeline for Development, Test, and Evaluation (DT&E)

The NeCTAR system is scheduled to complete its development and reach flight readiness within 4 years and 10 months, progressing from component-level procurement to full system-level validation. The major milestones and timeline are visualized in the chart above, with a start date in July 2025 and full system integration finalized by May 2030.

This timeline reflects a realistic and scalable approach to system maturation, integrating:

- Subsystem-level testing under lunar-analog conditions (e.g., TVAC and EMI),
- Hardware-in-the-loop simulations for autonomous control verification,
- And computational scaling models to extrapolate lab results to full lunar applications.

To ensure a viable path to lunar deployment within 3–5 years, each DT&E phase is designed to systematically raise NeCTAR's Technology Readiness Level (TRL), targeting TRL 6 by the end of subsystem testing and TRL 7 following complete system validation in a mission-representative environment.

Table 1. Major milestones in the DTE timeline for NeCTAR.

Milestone	Description	Elapsed Time (Months)
Components Procurement	Acquisition of materials, motors, sensors, and structural components.	T + 1.0
Sensor Calibration & Testing	Calibration of pressure sensors, thermocouples, and limit switches under cryogenic and vacuum conditions.	T + 4.0
Assembly & Subsystem Integration	Mechanical and electrical integration of NeCTAR subsystems.	T + 12.0
Engineering Unit Development	Engineering unit constructed with fully integrated cryogenic, mechanical, and sensor subsystems for system-level validation.	T + 30.0
Environmental Testing	Thermal vacuum and EMI testing to simulate lunar environment.	T + 42.0
Subsystem Verification & Validation	Subsystem-level functional tests and robustness assessments.	T + 48.0
Full System Verification & Final Integration	End-to-end system integration and full-scale validation under mission-representative conditions.	T + 56.0

7. Budget

The NeCTAR budget was developed using the NASA Cost Estimating Handbook (CEH) and aligned with real-world analogs such as cryogenic transfer lines, Artemis subsystem pricing, and past lunar payload missions. The budget separates key lifecycle phases: early technology maturation, system development, test and integration, and final mission infusion and long-term operations.

- Technology maturation ($1.2M) includes early prototyping and subsystem trade space evaluation.
- Development and integration ($11.1M combined) cover component builds, actuator and sensor configuration, and full-system environmental testing.
- Mission infusion costs ($1.0M) address requirements for TRL 7 qualification and documentation needed for NASA mission adoption.
- Launch costs ($25M) are benchmarked from CLPS and Artemis commercial delivery analogs, assuming a 150–200 kg payload.
- Surface operations ($21.3M over 10 years) average ~$2.13M/year, including comms, diagnostics, software maintenance, and off-nominal handling routines.

The applied cost margin of ~2.6% reflects hardware risk, materials variability, and uncertainties in lunar logistics. These values reflect a scalable, mission-ready architecture and provide sufficient margin for NASA adoption within 3–5 years.

Table 2. Comprehensive cost breakdown for the NeCTAR system.

Cost Category	**Description**	**Estimated Cost (1000$)**	**Cost Margin (1000$)**
Technology Maturation	Subsystem-level prototyping, trade studies, and initial lab tests	1,200	±40
System Development	Fabrication of flight units, actuator integration, sensor calibration	2,500	±75
Integration & Test	Assembly, cryogenic vacuum testing, EMI/thermal simulations	8,650	±80
Mission Infusion Prep	Flight certification, TRL advancement, regulatory documentation	1,000	±30
Launch & Delivery	Lunar payload packaging, delivery to staging site, launch to lunar surface	25,000	±1,000
Surface Operations (10 yrs)	Communications, health monitoring, telemetry handling, software updates	21,280	±320
Total Estimated Cost		**59,630**	**±1,545**

8. Mission Architecture Timeline

The NeCTAR mission follows a comprehensive concept-to-deployment timeline, progressing from early-stage development through integration with future lunar delivery missions. After concluding a 5-year development and verification phase, NeCTAR will be launched as part of a commercial lunar payload or Artemis cargo manifest in early 2031. Upon lunar surface deployment, the system will autonomously commission itself and begin cryogenic operations.

Over its 10-year expected lifespan, NeCTAR will support repeated bi-directional liquid oxygen transfer operations with minimal crew intervention. Its architecture is designed for durability, adaptability, and seamless integration with NASA's Human Landing System (HLS) infrastructure. Midlife evaluations and software updates ensure continued performance through the system's operational life, with decommissioning or transition occurring post-2041 based on mission needs and hardware condition.

Table 3. Full concept and mission architecture timeline for NeCTAR.

Phase	**Milestone**	**Timeframe**
Concept Design & Proposal	Initial design phase, trade studies	Completed (2024–2025)
Development & Testing	Component procurement,	2025–2030

	subsystem integration, environmental testing	
Flight Readiness Review (FRR)	TRL 7 confirmation, pre-launch qualification and system certification	Q4 2030
Launch Integration	Manifest selection and physical integration into a lunar cargo delivery mission (e.g., CLPS or Artemis)	Q1 2031
Lunar Launch & Delivery	Launch and surface delivery via cargo lander	Q2 2031
Surface Deployment & Commissioning	Initial power-up, diagnostics, and sensor calibration	Q2–Q3 2031
Autonomous Operations Phase	Bi-directional cryogenic transfer in support of HLS refueling	2031–2041
Midlife Assessment	Performance check, firmware updates, long-term diagnostic	2036 (Year 5)
End-of-Life / Transition	Evaluation of hardware integrity or replacement by next-gen system	2041+

9. Conclusion

The NeCTAR system addresses a critical need in NASA's long-term lunar strategy: enabling autonomous, safe, and robust cryogenic refueling in extreme environments. Through a modular architecture and an emphasis on dust mitigation, thermal integrity, and sensor-driven autonomy, NeCTAR provides a scalable and low-risk solution for sustained lunar operations. Our development approach combines proven hardware with iterative integration and test milestones, ensuring compatibility with the Human Landing System and future lunar infrastructure.

The proposed DT&E timeline advances NeCTAR to TRL 7 by 2030, with lunar deployment expected by 2031. Over a 10-year mission life, NeCTAR will significantly reduce crew burden, enhance safety, and demonstrate core technologies essential to future Mars and Gateway operations.

AGSL would like to extend its utmost appreciation towards the NIA, NASA, and their sponsors for the opportunity to technically develop such an interesting and unique concept in NeCTAR. AGSL would also like to recognize the invaluable oversight of her principal investigator, John Connolly, and the ever-present guidance of her former program manager, Alexander Duffy, and her current program manager, Shirish Pandam. Finally, AGSL thanks Texas A&M University for its dedication to space research, phenomenal education, and continued support of student-led organizations like AGSL.

References

[1] Hensley, M., Bhimji, W., and Cirillo, W., "A Review of In-Space Propellant Transfer Capabilities and Challenges for Missions Involving Propellant Resupply," NASA Technical Report NASA/TM-2020-5007997, 2020.

[2] Olhoeft, G.R., Pearce, G.W., and Strangway, D.W., "Magnetic and Dielectric Properties of Lunar Samples," *The Soviet-Am. Conf. on Cosmochem. of the Moon and Planets*, Pt. 1, NASA, Washington, January 1977.

[3] Gaier, J. R., "The Effects of Lunar Dust on EVA Systems During the Apollo Missions," NASA/TM—2005-213610, 2005. URL: https://ntrs.nasa.gov/citations/20050186598

[4] Sorongane, E.W., "The Classical Description of the Meissner Effect: Theory and Applications," *Open Journal of Applied Sciences*, Vol. 13, 2023, pp. 275–287. https://doi.org/10.4236/ojapps.2023.133022

[5] Tinkham, M., *Introduction to Superconductivity*, 2nd ed., Dover Publications, Mineola, NY, 2004.

[6] Lee, P. A., Nagaosa, N., and Wen, X.-G., "Doping a Mott Insulator: Physics of High-Temperature Superconductivity," *Reviews of Modern Physics*, Vol. 78, No. 1, 2006, pp. 17–85. https://doi.org/10.1103/RevModPhys.78.17

[7] Robinson, D. A., "Nickel and Its Alloys for Cryogenic Applications," *ASM Handbook*, ASM International, 1999.

[8] Afshar-Mohajer, N., Wu, C.Y., Moore, R., and Sorloaica-Hickman, N., "Design of an Electrostatic Lunar Dust Repeller for Mitigating Dust Deposition and Evaluation of its Removal Efficiency," *Journal of Aerosol Science*, Vol. 69, 2014, pp. 21–31. https://doi.org/10.1016/j.jaerosci.2013.11.005

[9] Wiesner, V. L., Wohl, C. J., King, G. C., Gordon, K. L., Das, L., and Hernandez, J. J., "Protective Coatings for Lunar Dust Tolerance," NASA/TM–20230003195, Langley Research Center, Hampton, VA, April 2023.

[10] ASM International, *Properties and Selection: Nonferrous Alloys and Special-Purpose Materials*, Vol. 2, *ASM Handbook*, ASM International, 1990.

[11] Gordon, J. S., "Cryogenic Material Properties Database," NASA Marshall Space Flight Center, 2001. URL: https://cryo.msfc.nasa.gov

[12] ASTM International, "ASTM E595-15: Standard Test Method for Total Mass Loss and Collected Volatile Condensable Materials from Outgassing in a Vacuum Environment," 2015.

[13] SAE International, "SAE J514: Hydraulic Tube Fittings," Society of Automotive Engineers, 1995.

[14] SAE International, "AS568: Aerospace Size Standard for O-Rings," Society of Automotive Engineers, 2001.

[15] SAE International, "AS5857: Gland Design, O-Ring and Other Elastomeric Seals, Static Applications," Society of Automotive Engineers, 2005.

[16] Chen, Q., Cui, Y., Sun, Q., Wu, Z., Yan, J., and Yang, X., "Development and Recent Progress of Hoses for Cryogenic Liquid Transportation," *Polymers*, Vol. 16, No. 7, 2024, Article 905. https://doi.org/10.3390/polym16070905

[17] Eagle Tube, "Optimal Metal Tubing for Medical Applications." URL: https://eagletube.com/resources/optimal-metal-tubing-for-medical

[18] Carter, W. B., and Paul, D. R., "Polymers for Cryogenic Applications," *Journal of Applied Polymer Science*, Vol. 97, No. 1, 2005, pp. 1–11. https://doi.org/10.1002/app.21551

[19] American Welding Society (AWS), *AWS D17.1/D17.1M:2024 – Specification for Fusion Welding for Aerospace Applications*, 2024.

[20] NASA, *NASA-STD-5006A: General Welding Requirements for Aerospace Materials*, NASA Technical Standards, 1997.

[21] American Society for Nondestructive Testing (ASNT), *NAS 410 and SNT-TC-1A: Qualification and Certification of Nondestructive Testing Personnel*, ASNT, 2024.

[22] Lundberg, L.B., "A Critical Evaluation of Molybdenum and its Alloys for Use in Space Reactor Core Heat Pipes," Los Alamos Scientific Lab, January 1981. https://doi.org/10.2172/6661144

[23] Bhat, B.N., Pandey, A.B., Tamirisakandala, S., et al., "Chapter 2: Aerospace Materials Characteristics," NASA/TM–20180001137, Marshall Space Flight Center, August 2018. https://doi.org/10.2514/4.104893

[24] MatWeb, LLC, "Titanium-Zirconium-Molybdenum (TZM) Alloy – Material Property Data," 2024. https://www.matweb.com

[25] Stanford Advanced Materials. (2024). *TZM Molybdenum Alloy Rods for Aerospace Use*. https://www.samaterials.com/molybdenum-alloys/92-tzm-products.html

[26] IOP Conference Series. (2024). *Low Cost, Simpler HTS Cable Conductors for Fusion Energy Systems*. https://iopscience.iop.org/article/10.1088/1757-899X/1241/1/012023/pdf

[27] "McCANNALOK SERIES CRYOGENIC HIGH PERFORMANCE BUTTERFLY VALVES TECHNICAL SALES MANUAL." Accessed: May 26, 2025. [Online]. Available: https://www.bray.com/docs/default-source/manuals-guides/technical-sales-guide/en_tsm_s4xcryo_20210319.pdf

[28] "Specification for Vacuum Insulated Piping General Fabrication, Testing and Purchasing." Accessed: May 26, 2025. [Online]. Available:

https://cryoworks.net/wp-content/uploads/2022/01/CDIENG-00118-Specification-for-Vacuum-Insulated-Piping-_002_-1.pdf

[29] J. Fesmire, A. Swanger, and C. Montreal, “ADVANCED CRYOGENIC INSULATION SYSTEMS,” 2019. Available: https://ntrs.nasa.gov/api/citations/20190030314/downloads/20190030314.pdf

[30] G. Bank, W. Virginia, G. Behrens, W. Campbell, D. Williams, and S. White, “NATIONAL RADIO ASTRONOMY OBSERVATORY Guidelines for the Design of Cryogenic Systems,” 1997. Accessed: May 26, 2025. [Online]. Available: https://www.gb.nrao.edu/electronics/edir/edir306.pdf

[31] “Design guidebook Delivery systems for cryogenic liquids in laboratories.” Accessed: May 26, 2025. [Online]. Available: https://www.beaconmedaes.com/content/dam/brands/beacon-medaes/documents/laboratory/guidebooks/BMed_Cryogenic_Design_Guide_%20Book_2021.pdf.coredownload.inline.pdf

[32] “Vacuum Jacketed/Insulated Piping for Cryogenic Liquids,” Cryogenic Equipment Solutions, Nov. 12, 2024. https://www.cryofab.com/products/cryogenic-transfer-lines/vacuum-jacketed-piping/ (accessed May 26, 2025).